*Int. J. Heat Mass Transfer.* Vol. 16, pp. 1199–1213. Pergamon Press 1973. Printed in Great Britain

# RADIATIVE HEAT TRANSFER BY FLOWING MULTIPHASE MEDIUM—PART III. AN ANALYSIS ON HEAT TRANSFER OF TURBULENT FLOW IN A CIRCULAR TUBE

**HIROSHI TAMEHIRO*, RYOZO ECHIGO and SHU HASEGAWA**
Department of Nuclear Engineering, Kyushu University, Fukuoka, Japan

(*Received* 28 *June* 1972)

**Abstract**—The heat transfer by gaseous suspension laminar flow of solid and/or liquid fine particles has been elucidated in the preceding papers by the authors when the thermal radiation predominates over other modes of heat transfer. In the present study an analysis is performed on the turbulent flow of the multiphase medium in a circular tube with constant wall temperature which is one of the most important problems in practice. The turbulent flow of gaseous suspension is, however, complicated in connection with the turbulent behaviors of the dispersed particles and the carrier fluid. Accordingly the tractable model has been employed by taking account of not only the radiative heat transfer to the particulate phase but the heat transfer between particles and surrounding fluid associated with turbulence. The reduced basic equations constitute simultaneous integro-differential equations which are solved numerically by the implicit finite difference method with iterative procedure of the radiative terms. Thereafter the calculated results on the temperature profiles and the heat transfer are examined in details.

## NOMENCLATURE

$A_p$, surface area of single particle $= \pi d_p^2$;
$B$, black body radiation $= (\sigma/\pi)T^4$;
$c_f, c_p$, specific heats of gas and particles;
$d_p$, particle diameter;
$f$, fanning friction factor;
$F(\tau_0)$, integral defined by equation (28);
$g_f$, total diffusivity function for gas;
$H(\tau_0\eta)$, integral defined by equation (12);
$h$, local heat transfer coefficient;
$h_p$, heat transfer coefficient between particle and gas;
$J_w$, radiation intensity from the wall $= (\sigma/\pi)T_w^4$;
$K(\tau_0\eta, \tau_0\eta_1)$, integrals defined by equation (12);
$k_f$, thermal conductivity of gas;
$M$, dimensionless parameter defined by equation (18);
$N_R$, radiation–conduction interaction parameter defined by equation (15);
$Nu_d$, Nusselt number on heat transfer between particle and surrounding gas defined by equation (1);
$Nu_{\xi,T}$, total local Nusselt number defined by equation (29);
$Nu_{\xi,C}$, local Nusselt number by convection defined by equation (30);
$Nu_{\xi,R}$, local Nusselt number by radiation defined by equation (31);
$n_p$, number of particles per unit volume;
$Pr$, Prandtl number $= \mu_f c_f/k_f$;
$q_C$, convective heat flux defined by equation (26);
$q_R$, radiative heat flux defined by equation (27);
$q_T$, total heat flux defined by equation (25);
$r$, radial coordinate;
$r^+$, dimensionless radial coordinate;
$R$, pipe radius;
$Re$, Reynolds number $= 2u_{fm}R/\nu_f$;
$S$, distance defined by equation (5);
$T_f, T_p$, temperatures of gas and particle;
$T_m$, cup-mixing mean temperature of

* Presently, Shin Nippon Iron and Steel Manufacturing Co.

flowing gaseous suspensions;
$T_0$, inlet temperature;
$T_w$, wall temperature;
$u_f, u_p$, axial velocities of gas and particles;
$u^+$, dimensionless axial velocity;
$U$, dimensionless axial velocity $= u/u_m$;
$V_p$, volume of a particle $= (\pi/6)d_p^3$;
$x$, axial coordinate;
$y^+$, dimensionless coordinate.

Greek symbols

$\Gamma$, thermal loading ratio defined by equation (14);
$\epsilon_p$, surface emissivity of particle;
$\varepsilon_{H,f}\varepsilon_{H,p}$, eddy diffusivities for heat in gaseous and particulate phase;
$\varepsilon_M$, eddy diffusivity for momentum;
$\eta$, dimensionless radial coordinate $= r/R$;
$\Delta\eta$, lattice spacing in the radial direction;
$\theta_f, \theta_p$, dimensionless temperatures of gas and particles;
$\theta_m$, dimensionless cup-mixing mean temperature of flowing gaseous suspensions defined by equation (34);
$\theta_{fm}, \theta_{pm}$, dimensionless temperatures of gas particles, defined by equations (32) and (33);
$\theta_0$, dimensionless inlet temperature;
$\Theta$, normalized dimensionless temperature $= (\theta - \theta_0)/(1 - \theta_0)$;
$\phi$, azimuthal angle shown in Fig. 2;
$\kappa$, absorption coefficient of dispersed particles defined by equation (7);
$\mu_f$, viscosity of gas;
$\nu_f$, kinematic viscosity of gas;
$\xi$, dimensionless axial coordinate $= (x/R)/RePr$;
$\Delta\xi$, lattice spacing in the axial direction;
$\rho_{dp}$, apparent density of dispersed particles;
$\rho_f, \rho_p$, densities of gas and particle material;
$\sigma$, Stefan–Boltzmann constant;
$\tau$, optical distance;
$\tau_0$, optical radius.

Suffixes

$C$, convection;
$dp$, dispersed phase;
$f$, gas (fluid);
$m$, mean value;
0, inlet;
$p$, particle;
$R$, radiation;
$T$, total;
$w$, wall;
1, dummy variable;
$\xi$, local.

## 1. INTRODUCTION

THE HEAT transfer by flowing suspensions has the following prominent characteristics [1, 2]:

(i) Flowing suspensions can fit for the operation at very high heat flux, due to the increased volumetric heat capacity of the medium.

(ii) At very high temperature, the radiative heat transfer can be improved as compared with gas alone because of the large absorptivity of the cloud of fine particles.

(iii) The improvement in the convective heat transfer with flowing suspensions over that with a pure gas can be expected due to the reduction of viscous sublayer thickness by the turbulence created by the random motion of particles in case of turbulent flow and so forth.

In the preceding studies the numerical analyses have been performed on the heat transfer with fully developed laminar flow of a suspension of fine particles between parallel plates [1] and in a circular tube [2].

In consequence, it is clarified that flowing gaseous suspensions are applicable to the heat transfer in high heat flux and high temperature systems and have the wide applications in industry, due to the basic nature discussed above.

The present analysis is concerned with the turbulent flow in a circular tube and it is, how-

ever, inevitable to exclude the detailed discussion on the turbulent behaviour of multiphase flow because of the veiled situation of the mechanism of multiphase turbulence. Hence, both physically and intuitively reasonable model is set up by taking account of the 'particulate character' of dispersed phase relating to the conductive, convective and radiative heat transfer.

## 2. ANALYSIS

### 2.1 *Description of the problem*

The coordinate system of the flow field is shown in Fig. 1. The mechanism of turbulence in

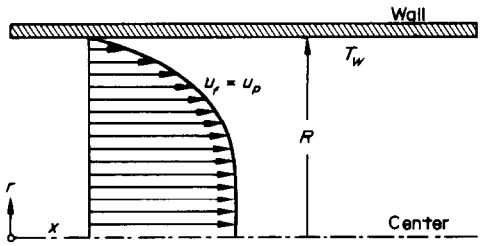


FIG. 1. Cylindrical coordinate system.

flowing gaseous suspensions of fine particles is so complicated that no information on the eddy diffusivities for the heat or momentum of the particles and the gas, either experimentally or analytically, is available so far. In the present analysis, therefore, it is assumed as done by Tien *et al.* [3] that the eddy diffusivity of the particles are equal to zero (that is, $\varepsilon_{H,p} = 0$) and the presence of particles has a negligible effect on the eddy diffusivity of the gas. It is readily seen that this is a close approximation to the actual system when the particles are very small and the loading ratio is less than or equal to unity.

The Nusselt number on the heat transfer between the particle and the gas, $Nu_d$ in equation (18), may be a function of the radial position $r$, due to the flow being turbulent near the particles, so that the Nusselt number $Nu_d$ is assumed in the following form

$$Nu_d = \frac{h_p d_p}{k_f} = 2 \cdot g_f. \tag{1}$$

This relationship has no theoretical or experimental ground except that this seems to be physically and intuitively acceptable. Here, $g_f = 1 + (\varepsilon_{H,f}/\nu_f)Pr$ and the value of $Nu_d = 2$ corresponds to the case by pure conduction in the viscous sublayer in which the turbulent fluctuations vanish.

In addition to the subjects discussed above the following assumptions are introduced into the analysis

(i) The pipe wall is isothermal ($T_w$ = constant) and black for thermal radiation.

(ii) The flow field of the two phases is hydrodynamically fully developed from the inlet and has a turbulent velocity distribution. The temperatures of the particles and the gas are the same at the inlet.

(iii) The pysical properties (such as $\rho$, $c$, $\mu$, $k$, etc.) are constant.

(iv) The particles are spheres of uniform size and thermal conductivity of which is large enough to neglect radial variation of temperature within the sphere.

(v) The particles are uniformly distributed throughout the pipe cross section, and emit and absorb thermal radiation as a gray fluid in local thermodynamic equilibrium, but do not scatter.* The gas is transparent for radiation.

(vi) The particles are sufficiently small and numerous to be considered as a continuum for thermal radiation.

(vii) The time-mean velocities of the two phases are equal and the presence of the particles has no effect on the velocity profile and the friction factor of the gas.

(viii) The agglomeration, chemical reaction of the particles and viscous dissipation are not considered.

* When the radiating medium is enclosed by solid surface(s) the isotropic scattering does not influence the radiative heat transfer, though the optical thickness of the medium is increased [4].

(ix) The energy transports by collisions among particles or with the wall are negligible as compared with those by conduction and radiation.

### 2.2 *The basic equations and their numerical solution*

On the foregoing postulation mentioned above, a heat balance in pipe flow yields the basic equations governing the temperature field. For the gas

$$c_f\rho_f u_f \frac{\partial T_f}{\partial x} + n_p h_p A_p (T_f - T_p) = \frac{c_f \rho_f}{r}\frac{\partial}{\partial r}\left\{ r\left(\frac{k_f}{c_f\rho_f} + \varepsilon_{H,f}\right)\frac{\partial T_f}{\partial r}\right\} \quad (2)$$

and for the particles

$$c_f \rho_{dp} u_p \frac{\partial T_p}{\partial x} + n_p h_p A_p (T_p - T_f) = \frac{c_p}{r}\frac{\partial}{\partial r}\left\{ r\varepsilon_{H,p}\rho_{dp}\frac{\partial T_p}{\partial r}\right\} - \operatorname{div} q_R. \quad (3)$$

The apparent density of the dispersed particles $\rho_{dp}$ is assumed constant everywhere and $\rho_{dp}$ is related to the density $\rho_p$ with the following equation

$$\rho_{dp} = \rho_p n_p V_p. \quad (4)$$

The first term in both equation (2) and equation (3) describes heat convected along the pipe; the second term is the heat transfer rate between the phases (an identical term in both equations) whilst the first term on the right hand side of the equations is the heat transferred radially due to eddy diffusion. For the gas, molecular conduction is assumed to contribute additively to radial heat transfer whereas there is considered to be no similar term for the particles.

Let us consider the geometrical configuration for the radiative heat flux in Fig. 2 where an arbitrary point is denoted by $(x, r)$ and a dummy variable point by $(x_1, r_1, \phi)$. The distance $S$ is then given by

$$S = \{(x_1 - x)^2 + r^2 + r_1^2 - 2rr_1\cos\phi\}^{\frac{1}{2}} \quad (5)$$

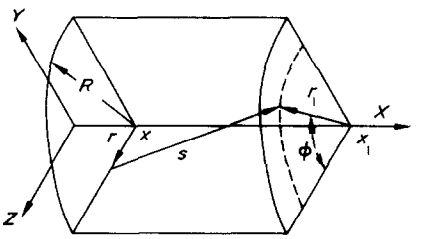


FIG. 2. Geometrical configuration for radiative heat flux.

and $S_w$ denotes the value of $S$ when $r_1 = R$.

Assuming the fluid to be in thermodynamic equilibrium and not to scatter, the divergence of the radiative heat flux vector [5]

$$-\operatorname{div} q_R = \kappa J_w \int_{-\infty}^{+\infty}\int_0^{2\pi} R(R - r)\exp\{-\tau(S_w)\}\frac{d\phi\, dx_1}{S_w^3} + \kappa^2 \int_0^R Br_1 \int_{-\infty}^{+\infty}\int_0^{2\pi} \exp\{-\tau(S)\}\times\frac{d\phi\, dr_1\, dx_1}{S^2} - 4\pi\kappa B \quad (6)$$

where $J_w$ is the intensity of the wall, $B$ is the blackbody radiation and $\tau(s)$ is the optical distance defined by

$$\tau(s) = \int_0^S \kappa(S_1)dS_1$$

The absorption coefficient $\kappa$ is given by the projected cross section of particles normal to the radiative flux

$$\kappa = \pi\left(\frac{d_p}{2}\right)^2 n_p \epsilon_p. \quad (7)$$

In deriving equation (6), the approximation of the one dimensional radiative heat flux is employed, based on the assumption that the radiative transfer in the axial direction is neglected as compared with the radial radiative heat transfer, i.e.

$$\frac{\partial q_{Rx}}{\partial x} \ll \frac{1}{r}\frac{\partial}{\partial r}(rq_{Rr}).$$

For the velocity distributions of the two phases, the expression developed by Reichardt [6] are used, that is for viscous sublayer, $y^+ \leqslant 5$

$$u^+ = y^+, \frac{\varepsilon_{M,f}}{\nu_f} \approx 0 \tag{8a}$$

for transition layer, $5 \leqslant y^+ \leqslant 30$

$$u^+ = -3{\cdot}05 + 5{\cdot}0 \ln y^+, \frac{\varepsilon_{M,f}}{\nu_f} = \frac{y^+}{5}\left(1 - \frac{y^+}{R}\right) - 1 \tag{8b}$$

for turbulent core, $y^+ \geqslant 30$

$$u^+ = 5{\cdot}5 + 2{\cdot}5 \ln\left[y^+ \frac{1{\cdot}5(1 + r/R)}{1 + 2(r/R)^2}\right],$$

$$\frac{\varepsilon_{M,f}}{\nu_f} = \frac{0{\cdot}4R^+}{6}\left[1 - \left(\frac{r}{R}\right)^2\right]\left[1 + 2\left(\frac{r}{R}\right)^2\right] \tag{8c}$$

where

$$u^+ = (u/u_m)/\sqrt{(f/2)}, \quad y^+ = (y/R)(Re/2)\sqrt{(f/2)}, \quad y^+ = R^+ - r^+$$

and the eddy diffusivity for heat $\varepsilon_{H,f}$ is calculated by use of the velocity distribution on the assumption that $\varepsilon_{H,f} \approx \varepsilon_{M,f}$. For brevity the boundary conditions are taken as follows

$$\begin{aligned} &r = R; && T_f = T_p = T_w \\ &r = 0; && \partial T_f/\partial r = \partial T_p/\partial r = 0 \\ &x = 0; && T_f = T_p = T_0. \end{aligned} \tag{9}$$

Strictly speaking, however, the temperature discontinuity between the heated wall and the particles at the wall has to be included in the boundary condition, due to the absence of the conduction term in equation (3). The results obtained with conditions of equation (9) underestimate the temperature gradient at the wall as compared with those obtained with the so-called "Radiation Slip" [7] condition, so that the heat-transfer characteristics are also underestimated. This effect is, however, expected to be small, because when the solid particles is travelling in the immediate neighborhood of the wall before hitting it, the temperature of the particles due to the local condition is very close to that of the wall.

After transforming equation (6) according to the method of Heaslet and Warming [8] and transforming equations (2) and (3) into dimensionless forms with the assumption that $U_f = U_p = U$, it was found after some manipulation,

for the gas

$$U\frac{\partial \theta_f}{\partial \xi} + M(\theta_f - \theta_p) = \frac{2}{\eta}\frac{\partial}{\partial \eta}\left(g_f \eta \frac{\partial \theta_f}{\partial \eta}\right) \tag{10}$$

and (when radial heat transfer by the particles neglected) for the particles

$$U\Gamma\frac{\partial \theta_p}{\partial \xi} + M(\theta_p - \theta_f) = \frac{2\tau_0^3}{N_R}H(\tau_0\eta) + \frac{2\tau_0^4}{N_R}\int_0^1 K(\tau_0\eta, \tau_0\eta_1)\,\eta_1\theta_p^4\,\mathrm{d}\eta_1 - \frac{2\tau_0^2}{N_R}\theta_p^4 \tag{11}$$

where

$$H(\tau_0\eta) = \int_1^\infty K_1(\tau_0 y)\, I_0(\tau_0\eta y)\frac{\mathrm{d}y}{y} \tag{12a}$$

$$K(\tau_0\eta, \tau_0\eta_1) = \begin{cases} \int_1^\infty K_0(\tau_0\eta y)\, I_0(\tau_0\eta_1 y)\,\mathrm{d}y & (\eta_1 < \eta) \\ \int_1^\infty K_0(\tau_0\eta_1 y)\, I_0(\tau_0\eta y)\,\mathrm{d}y & (\eta < \eta_1) \end{cases} \tag{12b}$$

$I_n(y)$ and $K_n(y)$ are modified Bessel functions of the first and second kind of $n$th order, respectively. The dimensionless parameters are

$$g_f = 1 + \frac{\varepsilon_{H,f}}{\nu_f}Pr \tag{13}$$

$$\Gamma = \frac{c_p\rho_{dp}u_{pm}}{c_f\rho_f u_{fm}} \tag{14}$$

$$N_R = \frac{\kappa k_f}{4\sigma T_w^3} \tag{15}$$

$$\tau_0 = \kappa R \tag{16}$$

$$\kappa = \pi\left(\frac{d_p}{2}\right)^2 n_p\epsilon_p \tag{17}$$

$$M = Nu_d \frac{2n_p A_p R^2}{d_p}. \tag{18}$$

The function $g_f$ is a characteristic parameter in turbulent flow and reduces to unity in laminar flow. The boundary conditions, then, become

$$\left.\begin{aligned} &\eta = 1; \quad \theta_f = \theta_p = 1 \\ &\eta = 0; \quad \partial\theta_f/\partial\eta = \partial\theta_p/\partial\eta = 0 \\ &\xi = 0; \quad \theta_f = \theta_p = \theta_0. \end{aligned}\right\} \tag{19}$$

Equations (10) and (11) constitute simultaneous nonlinear integrodifferential equations and it seems to be formidable to get the analytical solution by virtue of the high order nonlinearity. Therefore regarding equations (10) and (11) as the parabolic partial differential equation or its modified form, we calculate them numerically as the progressive type of problems by using the implicit finite difference method. In practical calculation, in order to achieve satisfactory accuracy near the wall, the comparatively small lattice spacing is used.

Considering the lattices in the radial direction as illustrated in Fig. 3 and assuming the $i$th surface temperature to be known and the $(i+1)$th surface temperature unknown, the derivatives

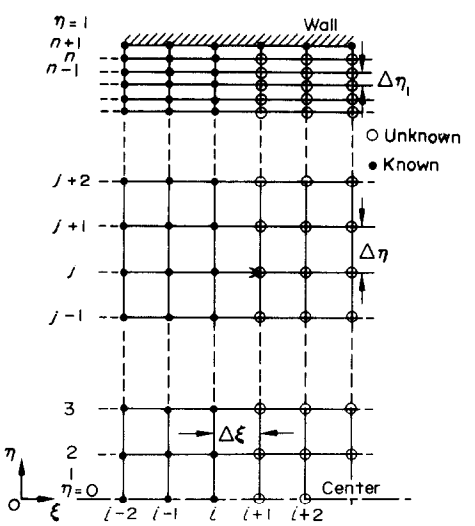


FIG. 3. Lattices of finite difference.

in equations (10) and (11) can be expressed by the following finite difference approximations.

$$\left.\begin{aligned} \frac{\partial\theta_f}{\partial\xi} &= \frac{\theta_f(i+1,j)-\theta_f(i,j)}{\Delta\xi} \\ \frac{\partial\theta_p}{\partial\xi} &= \frac{\theta_p(i+1,j)-\theta_p(i,j)}{\Delta\xi} \\ \frac{\partial\theta_f}{\partial\eta} &= \frac{\theta_f(i+1,j+1)-\theta_f(i+1,j-1)}{\Delta\eta+\Delta\eta_1} \\ \frac{\partial^2\theta_f}{\partial\eta^2} &= \frac{\theta_f(i+1,j+1)}{\Delta\eta(\Delta\eta+\Delta\eta_1)} - \frac{\theta_f(i+1,j)}{\Delta\eta\Delta\eta_1} \\ &\quad + \frac{\theta_f(i+1,j-1)}{\Delta\eta_1(\Delta\eta+\Delta\eta_1)}. \end{aligned}\right\} \tag{20}$$

The substitutions of equation (20) into equations (10) and (11), the approximation of integrals by trapezoidal formula and the replacement of $\theta_p(i+1,j)$ in integral terms of radiative heat flux in equation (11) with $\theta_p(i,j)$ as the zero-th order approximation yield

$$\begin{aligned} &U_j \frac{\theta_f(i+1,j)-\theta_f(i,j)}{\Delta\xi} + M_j\{\theta_f(i+1,j) \\ &\qquad - \theta_p(i+1,j)\} \\ &= 2\left(g_j' + \frac{g_j}{\eta_j}\right)\frac{\theta_f(i+1,j+1)-\theta_f(i+1,j+1)}{\Delta\eta+\Delta\eta_1} \\ &\quad + 4g_j\left\{\frac{\theta_f(i+1,j+1)}{\Delta\eta(\Delta\eta+\Delta\eta_1)} - \frac{\theta_f(i+1,j)}{\Delta\eta\Delta\eta_1}\right. \\ &\qquad \left. + \frac{\theta_f(i+1,j-1)}{\Delta\eta_1(\Delta\eta+\Delta\eta_1)}\right. \end{aligned} \tag{21}$$

$$\begin{aligned} &U_j\Gamma\frac{\theta_p(i+1,j)-\theta_p(i,j)}{\Delta\xi} + M_j\{\theta_p(i+1,j) \\ &\quad - \theta_f(i+1,j)\} = \frac{2\tau_0^3}{N_R}H(\tau_0\eta_j) + \frac{2\tau_0^4}{N_R}\frac{\Delta\eta}{2} \\ &\quad \times \{K(\tau_0\eta_j,\tau_0\eta_1)\eta_1\theta_p^4(i,1) \\ &\quad + K(\tau_0\eta_j,\tau_0\eta_m)\theta_p^4(i,m) \\ &\quad + 2\sum_{k=2}^{m-1} K(\tau_0\eta_j,\tau_0\eta_k)\eta_k\theta_p^4(i,k)\} \end{aligned}$$

$$+\frac{2\tau_0^4}{N_R}\frac{\Delta\eta_1}{2}\{K(\tau_0\eta_j,\tau_0\eta_m)\eta_m\theta_p^4(i,m)$$
$$+K(\tau_0\eta_j,\tau_0\eta_{n+1})\eta_{n+1}\theta_p^4(i,n+1)$$
$$+2\sum_{k=m+1}^{n}K(\tau_0\eta_j,\tau_0\eta_k)\eta_k\theta_p^4(i,k)\}$$
$$-\frac{2\tau_0^2}{N_R}\theta_p^4(i,j) \qquad (22)$$

where the prime denotes the differentiation with respect to $\eta$.

The values of $\eta_1$ and $\eta_{n+1}$ are equal to zero and unity, respectively and the spacing $\Delta\eta_1$ is equal to $\Delta\eta$ in equally spaced lattice range. Since equations (21) and (22) yield first order simultaneous equations of the $2n$-dimensions $[\theta_f(i+1,j),\ \theta_p(i+1,j);\ j=1\sim n]$ together with the same number of unknowns at the arbitrarily $(i+1)$-th cross section, one can get solutions immediately.

After obtaining $\theta_f(i+1,j)$, $\theta_p(i+1,j)$, $(j=1\sim n)$, these values are again substituted into $\theta_p(i,j)\,(j=1\sim n)$ on the right hand side in equation (22) as the 1st order approximation and then the similar computation is made repeatedly until the prescribed convergent condition for $k$th solutions $\theta_p^{(k)}$

$$\frac{\theta_p^{(k)}(i+1,j)-\theta_p^{(k-1)}(i+1,j)}{\theta_p^{(k)}(i+1,j)}<0{\cdot}0005 \qquad (23)$$

is satisfied. Thereafter advancing $\xi$ to the next step $\xi+\Delta\xi$, and the similar iterative calculations are repeated.

The ranges of dimensionless parameters covered here are as follows.

$$\Gamma = 0{\cdot}1\sim10{\cdot}0,\quad \tau_0 = 0{\cdot}0\sim3{\cdot}0$$
$$N_R = 0{\cdot}001\sim\infty,\quad Re = 5\times10^3\sim2\times10^4. \qquad (24)$$

## 3. DISCUSSION OF RESULTS

### 3.1 *Temperature profiles*

The typical results of the temperature profiles calculated here are illustrated in Figs. 4–8. The ordinate and the abscissa are normalized to be $\Theta=[(\theta-\theta_0)/(1-\theta_0)]$ and $y/R$, respectively.

*Table 1*

| Para. \ Fig. | 4 | 5 | 6 | 7 | 8 |
|---|---|---|---|---|---|
| $N_R$ | 0·01 | 0·01 | — | 0·01 | 0·01 |
| $\Gamma$ | 1·0 | 1·0 | 1·0 | — | 1·0 |
| $\tau_0$ | 1·0 | 1·0 | 1·0 | 1·0 | — |
| $Re$ | $10^4$ | — | $10^4$ | $10^4$ | $10^4$ |

$M=8\times10^3 g_f$, $Pr=1$, $\theta_0=0{\cdot}5$.

The values of parameters shown in each figure are listed in Table 1, in which the value $M=8000g_f$ corresponds to the case of $Nu_d=2g_f$ and $d_p=10\mu$. The general trend on the temperature profiles are as follows:

(i) In the vicinity of the heated wall the temperature gradient becomes steeper due to the presence of fine particles and as a result the convective heat transfer is promoted while in the central core of a pipe the gas temperature is increased by the heat transfer from fine particles, which absorb thermal radiation.

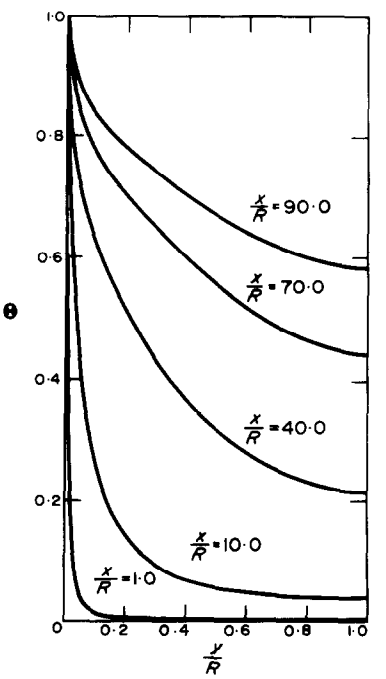


FIG. 4. Temperature profiles vs $y/R$ (effect of $x/R$).

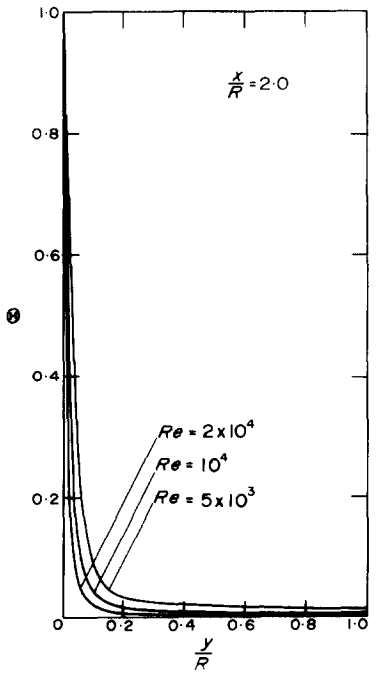


FIG. 5(a). Temperature profiles vs $y/R$ (effect of $Re$).

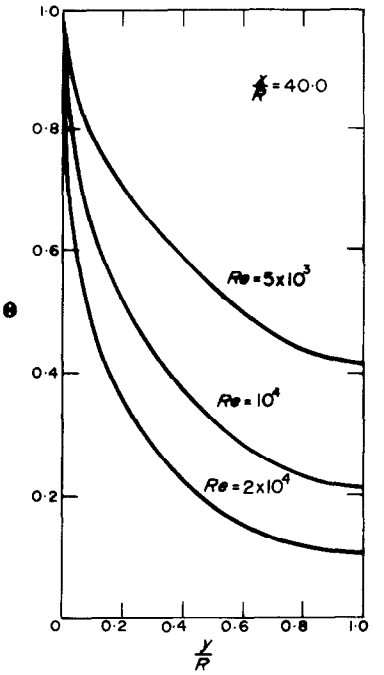


FIG. 5(c). Temperature profiles vs $y/R$ (effect of $Re$).

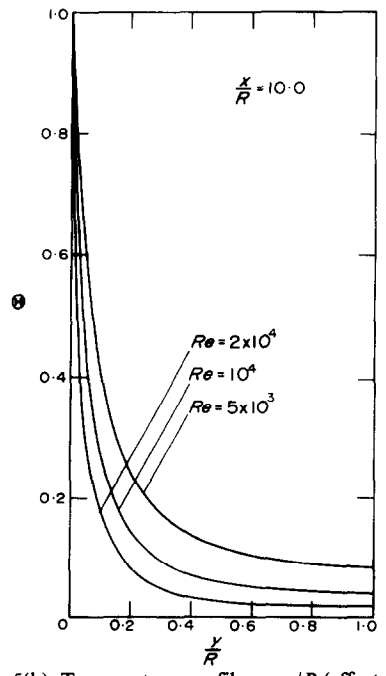


FIG. 5(b). Temperature profiles vs $y/R$ (effect of $Re$).

(ii) The temperature difference of the two phases cannot be found throughout the pipe radius by virtue of the fluid turbulence near the particles and this situation does not vary with axial distance $x/R$.

Figures 4 and 5 show the variations of the temperature profiles with axial distance $x/R$ and Reynolds number $Re$, respectively.

The lower temperature rises with increasing $Re$ are ascribed to the increment of the volumetric flow rate, when same fluid is used. Since the fraction occupied by convective heat transfer in total heat-transfer rate reduces as the radiation contribution increases, it is rather favorable to employ laminar flow in the very-high temperature system but a certain device may be required to eliminate the temperature difference of the two phases. Additionally it appears that the radiative heat transfer is not so effected by the variations of Reynolds number and therefore it is almost independent of the flow field.

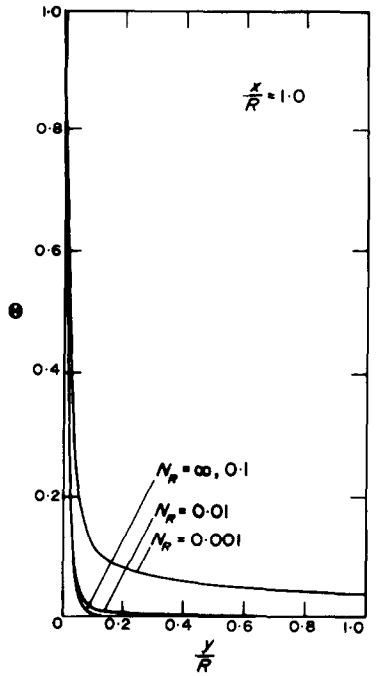


FIG. 6(a). Temperature profiles vs $y/R$ (effect of $N_R$).

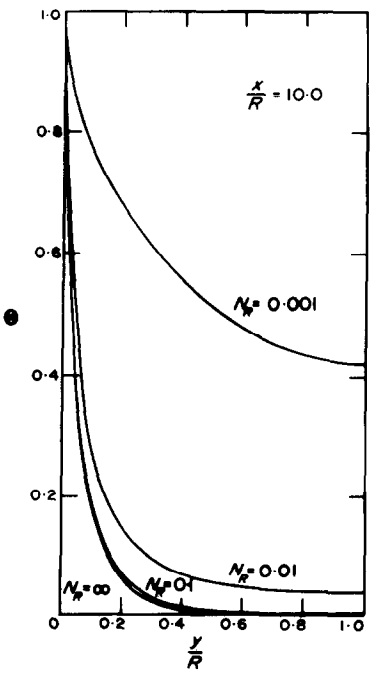


FIG. 6(b). Temperature profiles vs $y/R$ (effect of $N_R$).

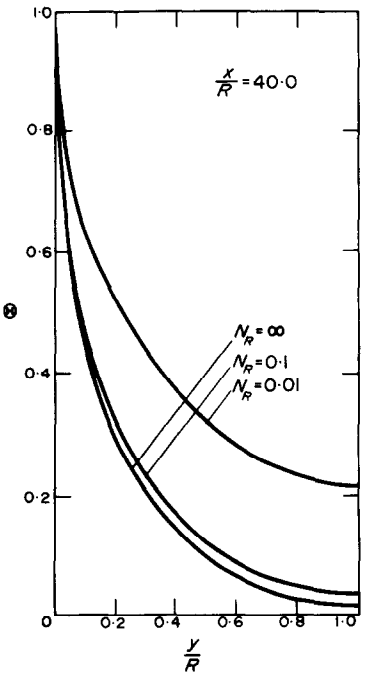


FIG. 6(c). Temperature profiles vs $y/R$ (effect of $N_R$).

Figures 6(a)–(c), which correspond to axial distance $x/R = 1$, 10, 40, respectively illustrate the effect of parameter $N_R$ on the temperature profiles.

In the case of $N_R = 0{\cdot}001$ in which radiative heat transfer is pronouncedly predominated, for laminar flow of gaseous suspension the considerably large temperature difference between carrier fluid and dispersed particles yields [2] so that this is not favorable from the viewpoint of the effective heating of the gas. For turbulent flow, however, the temperature difference between two phases is negligible due to the turbulence and this fact is favorable for the practical purpose.

The careful examination on the numerical results shows that:

(i) the temperature of the particles is higher in the central core while in the proximity of the wall it is lower than that of the gas and the intersection of both temperature profiles moves toward the wall with decreasing

$N_R$ (larger radiation contribution) and increasing $x/R$.

(ii) the temperature difference increases with decreasing $N_R$ and does not appreciably vary with $x/R$.

(iii) the temperature gradient at the wall reduces as the parameter $N_R$ decreases.

These tendiencies are also found in laminar flow [2].

Figures 7(a)–(c), which correspond to axial distance $x/R$ = 1, 10, 40, respectively, illustrate the effect of the loading ratio $\Gamma$ on the temperature profiles. Here the variation of the loading ratio $\Gamma$ under the fixed optical radius $\tau_0$ can be achieved by either using the different size of particles or other kind of particle (different emissivity $\epsilon_p$). The temperature difference decreases with increasing $\Gamma$ and in turbulent flow it is almost negligible over the range calculated here ($\Gamma$ = 0·1–10).

For large $\Gamma$ the development of the temperature

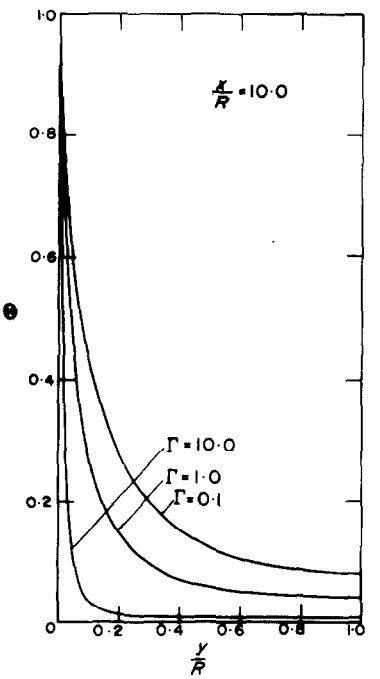


FIG. 7(b). Temperature profiles vs $y/R$ (effect of $\Gamma$)

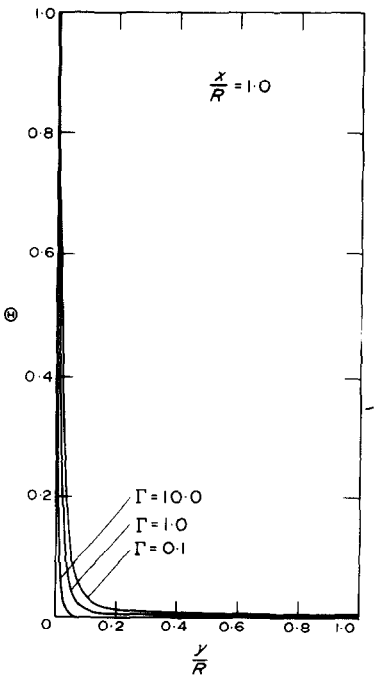


FIG. 7(a). Temperature profiles vs $y/R$ (effect of $\Gamma_R$).

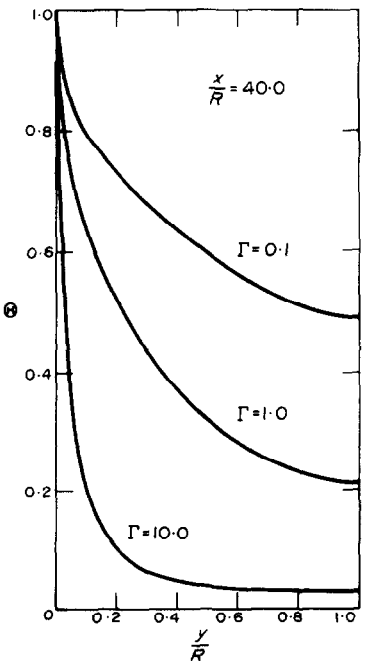


FIG. 7(c). Temperature profiles vs $y/R$ (effect of $\Gamma$).

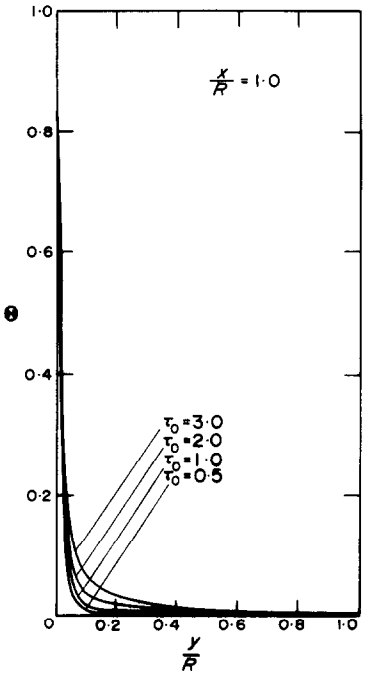


FIG. 8(a). Temperature profiles vs $y/R$ (effect of $\tau_0$).

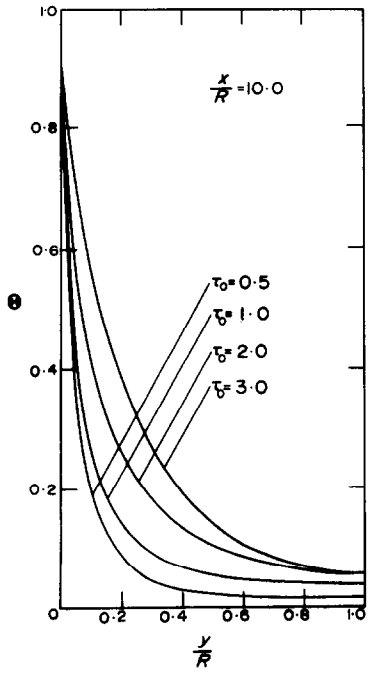


FIG. 8(b). Temperature profiles vs $y/R$ (effect of $\tau_0$).

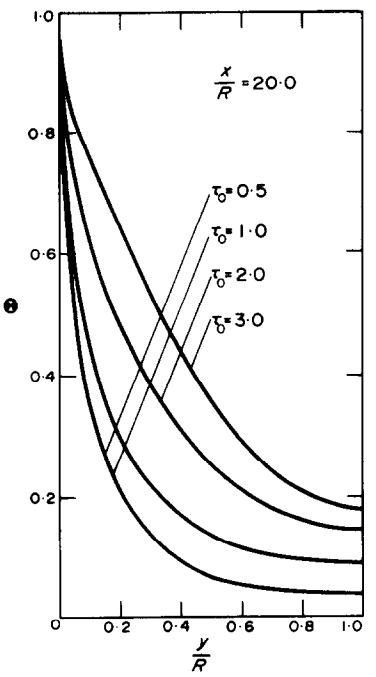


FIG. 8(c). Temperature profiles vs $y/R$ (effect of $\tau_0$).

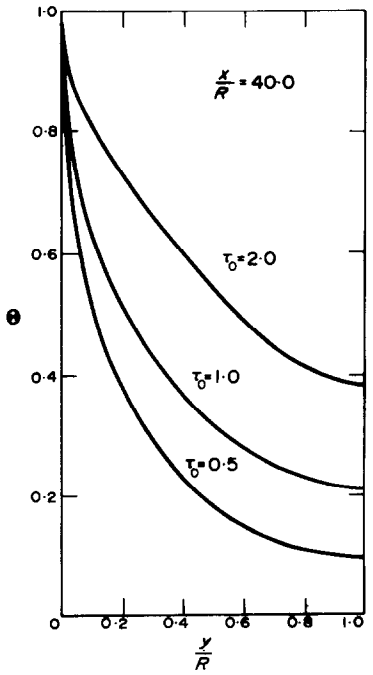


FIG. 8(d). Temperature profiles vs $y/R$ (effect of $\tau_0$)

field is decelerated due to the increased heat capacity of flowing suspensions and, in consequence, thermal entry lengths are considerably prolonged. The large $\Gamma$ is, however, disadvantageous from the viewpoint of the effective heating of the gas. It seems that the case of $\Gamma = 10$ slightly digresses from the present analysis.

Figures 8(a)–(d), which correspond to axial distance $x/R = 1$, 10, 20 and 40, respectively, illustrate the effect of the optical radius $\tau_0$ on the temperature profiles. The radiative heat transfer characteristics of the particles are very excellent and the optical radius $\tau_0$ can be varied with ease in a suspension flow system, as mentioned before, so that it is of great importance to examine the effect of the optical radius $\tau_0$ on the temperature profiles. References to Fig. 8 reveal the fact that when $\tau_0 = 3$ the temperature rises considerably near the wall as compared with those of smaller $\tau_0$ while in central core it is rather lower than that of $\tau_0 = 2$ at inlet section, but exceeds it easily as the fluid flows down-stream, because the eddy diffusivity for heat in turbulent flow regime may probably play an important role along the radial direction. In laminar flow when the optical length of the flowing medium is deep from the heat surface the so-called radiation shield occurs, that is, the radiation energy cannot penetrate to the central core and, in consequence, the excursion of temperature profile from parabolic becomes considerable due to lower transport ability for heat along radius direction without turbulence.

When $\tau_0 = 0{\cdot}5$, the temperature rise is comparatively small throughout the flow channel in spite of the large radiation contribution ($N_R = 0{\cdot}01$), since radiation easily penetrates through the fluid without absorption.

### 3.2 *Heat transfer*

The total, convective and radiative heat fluxes at the wall and the local Nusselt numbers are defined by the following equations.

$$q_T = q_C + q_R \tag{25}$$

$$q_C \frac{R}{k_f T_w} = \left.\frac{\partial \theta_f}{\partial \eta}\right|_{\eta=1} \tag{26}$$

$$q_R \frac{R}{k_f T_w} = \frac{\tau_0^2}{N_R} F(\tau_0) - \frac{\tau_0^3}{N_R} \int_0^1 \theta_p^4 \eta_1 H(\tau_0 \eta_1)\, \mathrm{d}\eta_1 \tag{27}$$

where

$$F(\tau_0) = \int_1^\infty K_1(\tau_0 y)\, I_1(\tau_0 y) \frac{\mathrm{d}y}{y^2} \tag{28}$$

$$Nu_{\xi,T} = \frac{h_\xi 2R}{k_f} = \frac{q_T \cdot 2R}{k_f (T_w - T_m)} = Nu_{\xi,C} + Nu_{\xi,R} \tag{29}$$

$$Nu_{\xi,C} = \frac{q_c \cdot 2R}{k_f (T_w - T_m)} \tag{30}$$

$$Nu_{\xi,R} = \frac{q_R \cdot 2R}{k_f (T_w - T_m)}. \tag{31}$$

The dimensionless cup-mixing mean temperature of the gas, the particles and the two phases are

$$\theta_{fm} = \int_0^1 U\theta_f \eta \, \mathrm{d}\eta \Big/ \int_0^1 U\eta \, \mathrm{d}\eta \tag{32}$$

$$\theta_{pm} = \int_0^1 U\theta_p \eta \, \mathrm{d}\eta \Big/ \int_0^1 U\eta \, \mathrm{d}\eta \tag{33}$$

$$\theta_m = \int_0^1 U(\theta_f + \Gamma\theta_p)\eta \, \mathrm{d}\eta \Big/ (1+\Gamma) \int_0^1 U\eta \, \mathrm{d}\eta = \frac{\theta_{fm} + \Gamma\theta_{pm}}{1+\Gamma} \tag{34}$$

respectively. Equations (30) and (31) can be then rewritten as follows

$$Nu_{\xi,C} = 2 \left.\frac{\partial \theta_f}{\partial \eta}\right|_{\eta=1} \Big/ (1 - \theta_m) \tag{35}$$

$$Nu_{\xi,R} = 2 \left\{ \frac{\tau_0^2}{N_R} F(\tau_0) - \frac{\tau_0^3}{N_R} \int_0^1 \theta_p^4 \eta_1 H(\tau_0 \eta_1) \mathrm{d}\eta_1 \right\} / (1 - \theta_m). \tag{36}$$

The total Nusselt number $Nu_{\xi,T}$ vs axial distance $x/R$ is shown for various representative parameters in Fig. 9. The parameters of each curves in Figs. 9 and 10 are listed in Table 2. The qualitative tendency is analogous to that of the laminar flow.

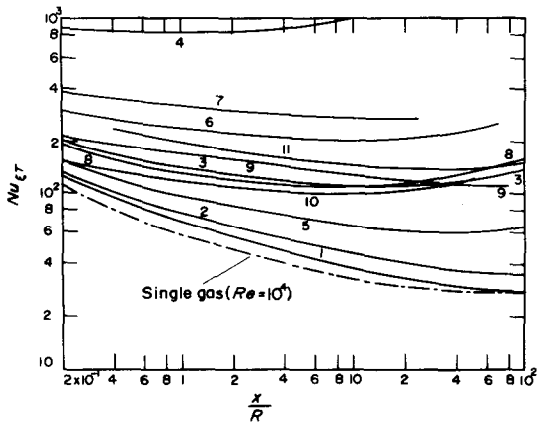


FIG. 9. Total Nusselt number $Nu_{\xi,T}$ vs $x/R$.

As being found from the reference to a chained line the Nusselt number of single gas by pure conduction is slightly lower than that obtained from the exact solution (not reproduced here), though the errors are tolerably small. This is due to the fact that the temperature gradient at the wall included in the convective Nusselt number is calculated by using the very small numerical values in finite difference approximation. Since the error is considered as the limitation of the accuracy of finite difference method, the smaller lattice spacing is not employed.

The cup-mixing mean temperature, the temperature profiles and the convective Nusselt number are, however, expected to be substantially correct and the satisfactory accuracy may be obtained when the radiative heat transfer predominates over the convective heat transfer.

The Nusselt number $Nu_{\xi,T}$ decreases to a certain minimum and turns to increase beyond this point, which is a striking feature when the radiation effect is included and implies that the temperature field cannot be fully developed even in a downstream. In connection with the fact that the minimum of $Nu_{\xi,T}$ moves toward the inlet of a pipe as $N_R$ or $\Gamma$ decreases, the reason why $Nu_{\xi,T}$ takes a minimum can be also considered that when the radiation effect is included the cup-mixing mean temperature $\theta_m$ of the two phases rapidly increases as compared with the reduction of the heat flux as the fluid flows downstream. The effect of parameters $\tau_0$ and $N_R$ on $Nu_{\xi,T}$ is considerable and $Nu_{\xi,T}$ increases with increasing $\tau_0$ and decreasing $N_R$. The effect of $\Gamma$ is, however, small while that of $Nu_{\xi,C}$ is appreciably large.

The cup-mixing mean temperature $\theta_m$ vs axial distance $x/R$ is shown for various parameters in Fig. 10. A chained line curve denotes the single gas flow at $Re = 10^4$. Here it must be noted that when $\Gamma = 1$ and 10 the heat capacities of flowing media are twice, and eleven times as

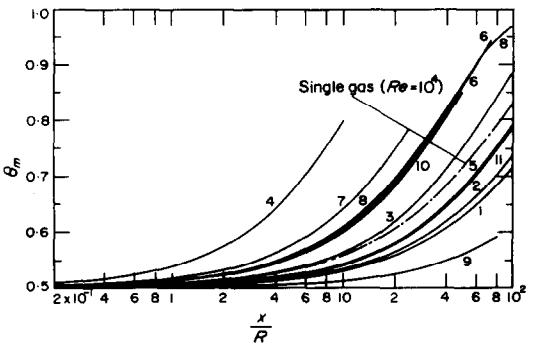


FIG. 10. Cup-mixing mean temperature of the two phases vs $x/R$.

*Table 2*

| Para. \ No | 1 | 2 | 3 | 4 | 5 | 6 | 7 | 8 | 9 | 10 | 11 |
|---|---|---|---|---|---|---|---|---|---|---|---|
| $N_R$ | $\infty$ | 0·1 | 0·01 | 0·001 | 0·01 | 0·01 | 0·01 | 0·01 | 0·01 | 0·01 | 0·01 |
| $\Gamma$ | 1·0 | 1·0 | 1·0 | 1·0 | 1·0 | 1·0 | 1·0 | 0·1 | 10·0 | 1·0 | 1·0 |
| $\tau_0$ | — | 1·0 | 1·0 | 1·0 | 0·5 | 2·0 | 3·0 | 1·0 | 1·0 | 1·0 | 1·0 |
| $Re$ | $10^4$ | $10^4$ | $10^4$ | $10^4$ | $10^4$ | $10^4$ | $10^4$ | $10^4$ | $10^4$ | $5\times10^3$ | $2\times10^4$ |

$M = 8 \times 10^4\, g_f$, $Pr = 1, \theta_0 = 0{\cdot}5$.

large as that of single gaseous phase flow, respectively. Therefore, in spite of the large contribution of radiation, the temperature of $\Gamma = 10$ is lower than that of single gaseous phase flow.

Finally the calculation is performed with the parameters of eddy diffusivity for heat in particulate phase to that in fluid phase, $\varepsilon_{H,p}/\varepsilon_{H,f}$ to be equal 0·2/0·8 and the result shows that the heat transfer characteristic is almost unchanged.

## 4. CONCLUSIONS

Combined radiation and turbulent forced convective heat transfer by gaseous suspensions of fine particles is examined and the effects of various parameters on the temperature profiles and the heat-transfer characteristics are discussed in some detail. The important conclusions obtained here are as follows:

(1) The heat-transfer characteristics can be remarkably improved by flowing suspensions; that is, the temperature gradient becomes steeper due to the presence of particles in the vicinity of the wall, while in the central core of a pipe the gas temperature is elevated by the heat transfer from the fine particles which absorb radiation.

(2) When the radiation effect is included, there exists no fully developed temperature profile even in a downstream; that is the Nusselt number decreases to a certain minimum and thereafter tends to increase with axial distance $x/R$. Additionally the temperature profile deviates from that by pure conduction. These behaviors are considered to be connected with each other.

(3) In a suspension flow system many applications are considered in its use, so that it should be necessary to examine the heat-transfer mechanism by taking account not only of the heat-transfer characteristics but also of the cup-mixing mean temperature.

The three results above also hold for laminar flow [1, 2].

(4) The radiative heat transfer does not appreciably change with Reynolds number and therefore is independent of the flow field. Since, at very high temperature, the fraction occupied by convective heat transfer in total heat-transfer rate is small as compared with that occupied by radiative heat transfer, it is rather favorable to employ laminar flow from the viewpoint of pumping power for circulation.

(5) In turbulent flow, the temperatures of the two phases are indistinguishable, so that it seems possible to perform the analysis under the condition of $T_f \simeq T_p$.

(6) In contrast to the laminar flow the radiation shield for comparatively large optical radius is not appeared which might be attributed to the eddy diffusivity in turbulent flow.

The numerical computation in this paper has been performed at the Computer Center, Kyushu University by FACOM 230–60.

## REFERENCES

1. R. ECHIGO and S. HASEGAWA, Radiative heat transfer by flowing multiphase medium—Part I. An analysis on heat transfer of laminar flow between parallel flat plates, *Int. J. Heat Mass Transfer* **15**, 2519–2534 (1972).
2. R. ECHIGO, S. HASEGAWA and H. TAMEHIRO, Radiative heat transfer by flowing multiphase medium—Part II. An analysis on heat transfer of laminar flow in an entrance region of circular tube, *Int. J. Heat Mass Transfer* **15**, 2595–2610 (1972).
3. C. L. TIEN, Heat transfer by a tubulent flowing fluid–solids mixture in a pipe, *J. Heat Transfer* **83C**. 183–188 (1961).
4. R. VISKANTA, Radiation transfer and interaction of convection with radiation heat transfer, *Advances in Heat Transfer*, Vol. 3. Academic Press, New York (1966).
5. B. E. PEARCE and A. F. EMERY, Heat transfer by thermal radiation and laminar forced convection to an absorbing fluid in the entry region of a pipe, *J. Heat Transfer* **92C**, 221–230 (1970).
6. H. REICHARDT, *Z. Angew. Math. Mech.* **31**, 208 (1951).
7. E. M. SPARROW and R. D. CESS, *Radiation Heat Transfer*, p. 267. Brooks/Cole, Belmont, Calif. (1966).
8. M. A. HEASLET and R. F. WARMING, Theoretical prediction of radiative transfer in a homogeneous cylindrical medium, *J. Quant. Spectrosc. Radiat. Transfer* **6**, 751–774 (1966).

## RAYONNEMENT THERMIQUE PAR UN MILIEU MULTIPHASIQUE EN ECOULEMENT—III. ANALYSE DU TRANSFERT THERMIQUE D'UN ECOULEMENT TURBULENT DANS UN TUBE CIRCULAIRE

**Résumé**—Le transfert thermique par l'écoulement laminaire d'une suspension gazeuse de fines particules solides et (ou) liquides, a été traité dans les articles précédents par les auteurs, quand le rayonnement thermique prédomine sur les autres modes de transfert. Dans la présente étude, on a conduit une analyse de l'écoulement turbulent d'un milieu multiphasique dans un tube circulaire à température pariétale constante, l'un des problèmes pratiques les plus importants.

Cependant l'écoulement turbulent de la suspension gazeuse est compliqué par les comportements turbulents des particules dispersées et du fluide porteur. En conséquence le modèle considéré a été employé en tenant compte non seulement du transfert thermique par rayonnement à la phase dispersée mais du transfert thermique, entre les particules et le fluide environnant, associé à la turbulence. Les équations réduites fondamentales constituent des équations intégro-différentielles simultanées qui sont numériquement résolues par la méthode implicite aux différences finies avec un processus itératif des termes de rayonnement. Les résultats calculés sur les profils de température et le transfert thermique sont ensuite examinés en détail.

## WÄRMETRANSPORT DURCH STRAHLUNG IN EINEM FLIESSENDEN VIELPHASIGEN MEDIUM
## TEIL III: EINE UNTERSUCHUNG DES WÄRMETRANSPORTES BEI TURBULENTER STRÖMUNG IN EINEM KREISFÖRMIGEN ROHR

**Zusammenfassung**—In den vorangegangenen Arbeiten wurde der Wärmetransport bei laminarer Strömung einer gasförmigen Suspension fest und/oder flüssiger kleiner Teilchen für den Fall behandelt, dass die thermische Strahlung die anderen Arten des Wärmetransportes überwiegt. In dieser Arbeit wird eine Untersuchung der turbulenten Strömung des Vielphasenmediums in einem kreisförmigen Rohr mit konstanter Wandtemperatur durchgeführt. Dies ist für die Praxis eines der wichtigsten Probleme. Bei der turbulenten Strömung einer gasförmigen Suspension ist jedoch die Verbindung des turbulenten Verhaltens der dispergierten Teilchen und des Trägerfluids kompliziert. Daher wurde das Modell so angewandt, dass nicht nur der Wärmeübergang durch Strahlung auf die jeweilige Phase berücksichtigt wurde, sondern auch der turbulente Wärmeübergang zwischen den Teilchen und der umgebenden Flüssigkeit. Die reduzierten Basisgleichungen bilden simultane Integraldifferentialgleichungen, die numerisch durch die implizite Methode der endlichen Differenzen gelöst wurden, mit Iteration der Strahlungsterme. Die berechneten Ergebnisse für die Temperaturprofile und den Wärmeübergang werden noch im Detail geprüft.

## ЛУЧИСТЫЙ ТЕПЛООБМЕН ПРИ ТЕЧЕНИИ МНОГОФАЗНОЙ СРЕДЫ. 3. АНАЛИЗ ТЕПЛООБМЕНА ПРИ ЛАМИНАРНОМ ТЕЧЕНИИ В КРУГЛОЙ ТРУБЕ

**Аннотация**—Перенос тепла при ламинарном течении газовзвесей твердых и/или жидких мелких частиц описан в ранее опубликованных авторами работах по тепловому излучению, превалирующему над всеми другими видами переноса тепла. В данной работе рассматривается турбулентное течение многофазной среды в круглой трубе при постоянной температуре стенки, что является очень важной практической задачей. Однако турбулентное течение газовзвесей усложняется в связи с различным поведением дисперсных частиц и среды. В соответствии с этим используется удобная модель, учитывающая не только лучистый перенос тепла к дисперсной фазе, но и теплообмен между частицами и окружающей жидкостью, связанный с турбулентностью. Приведенные основные уравнения являются системой интегро-дифференциальных уравнений, которые решаются численно с помощью неявных конечно-разностных схем методом итерации членов, учитывающих излучение. Проведен детальный анализ рассчитанных распределений температуры и теплообмена.